Influence of chemical reduction on the particular number densities of light-induced small electron and hole polarons in nominally pure $LiNbO_3$

C. Merschjann,* B. Schoke, and M. Imlau
Fachbereich Physik, Universität Osnabrück, D-49069 Osnabrück, Germany
(Received 24 April 2007; published 10 August 2007)

The influence of chemical reduction on the particular number densities of light-induced free small Nb_{Nb}^{4+} electron polarons, bound small Nb_{Li}^{4+} electron polarons, bound small Nb_{Li}^{4+}:Nb_{Nb}^{4+} electron bipolarons, and bound small O^- hole polarons is investigated in nominally pure, congruently melting $LiNbO_3$ by means of excited-state absorption spectroscopy. Characteristic changes in the sign of the light-induced absorption in the blue-green spectral range and distinctive dependencies on the pump beam intensity reflect the increasing contribution of electron polarons generated upon single intense ns-laser pulses at $\lambda = 532$ nm with increasing degree of reduction. The entire data set including its time dependence and spectral properties is consistently explained within a model taking into account the presence of all four types of electron and hole polarons, and residual $Fe^{2+/3+}$ impurities. The model includes one- and two-photon excitation processes for polaron generation, optical gating of bipolarons, and direct and two-step polaronic recombination processes. Our results indicate a mutual independence of two-photon hole polaron generation and one-photon dissociation processes of bipolarons, at least for moderate degrees of reduction.

DOI: 10.1103/PhysRevB.76.085114 PACS number(s): 71.38.−k, 71.38.Ht, 71.38.Mx, 71.55.−i

I. INTRODUCTION

Small polarons in general, and in particular their optical absorption properties, have attracted attention for more than 40 years. They are of increasing importance for the field of photorefraction, e.g., for two-color holography in $LiNbO_3$.[1–4] On the other hand, photochromic effects—i.e., light-induced absorption changes α_{li} related to small-polaron formation—are an issue for nonlinear-optical oxide crystals, since they strongly affect the performance of laser systems, eventually resulting in catastrophic damage of optical devices.[5] Among the materials showing photochromic effects are LiB_3O_5,[6] $KTiOPO_4$,[7] $LiTaO_3$,[8] $KNbO_3$,[9] and $LiNbO_3$.[10] For all of the oxides named here a contribution of small polarons to the light-induced absorption was assumed, for the latter three their existence is currently widely accepted.

A polaron is a charge carrier together with the lattice distortion it induces in a polar material.[11–13] We speak of a small polaron if the carrier is restricted to a single lattice site and the corresponding distortion mainly involves the bonds to nearest-neighbor sites.[11–13] In the case of lithium niobate, at least four different kinds of intrinsic small polarons could be identified, yielding characteristic absorption bands in the visible to near-infrared spectral range.[14–17] This variety of intrinsic photochromic centers makes $LiNbO_3$ an ideal candidate for investigations of (light-induced) small polarons, the related absorption changes, and interaction kinetics. Congruently melting, nominally pure $LiNbO_3$ shows a Li deficiency, which is partly compensated by Nb on Li sites.[18] Chemical reduction by vacuum annealing leads to the formation of stable small Nb_{Li}^{4+}:Nb_{Nb}^{4+} electron bipolarons with an absorption band centered at 2.5 eV (500 nm, cf. Fig. 1).[15] It is well known that the number density of bipolarons can be adjusted by different reduction treatments. Furthermore they are dissociated by light in the blue-green spectral range ("gating"),[2] resulting in the generation of metastable free and bound small electron polarons (Nb_{Nb}^{4+} and Nb_{Li}^{4+}).[19] The absorption of these is centered at 1.0 eV (1250 nm) (Ref. 17) and 1.6 eV (760 nm),[15] respectively. In unreduced samples a transient light-induced absorption upon intense pulsed green illumination was also observed and assigned to the light-induced generation of Nb_{Li}^{4+} and bound small O^- hole polarons.[20] The latter yield an absorption similar in shape and position to that of the bipolarons.[14,21]

Not much is known, however, about the relation between the number densities of the respective light-induced polaronic states and the degree of chemical reduction. In particular, this relation is of interest if the corresponding phenomena of the light-induced absorption are taken into account: For instance, a light-induced absorption appears in nominally pure, unreduced $LiNbO_3$ crystals in the blue-green spectral range whereas a pronounced light-induced transparency is found in the same samples after chemical reduction.

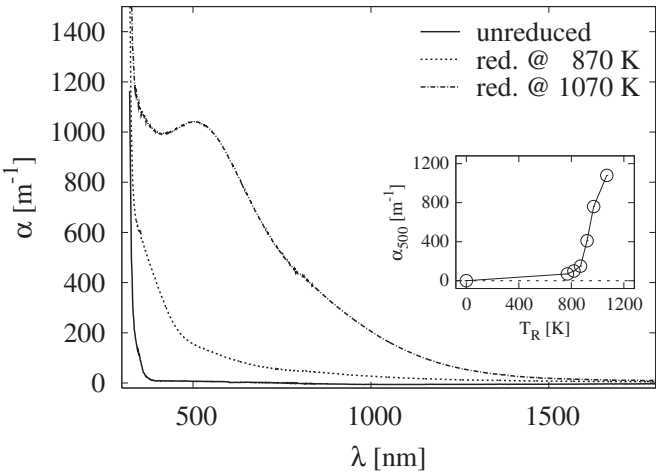

FIG. 1. Steady-state absorption of selected $LiNbO_3$ samples used in this work. The corresponding absorption values at 500 nm (α_{500}) are listed in Table I. The dependence of α_{500} on the reduction temperature is shown in the inset.

It is the aim of the present work to shed light on this striking influence of the chemical reduction on the light-induced absorption, i.e., the number densities of the particular electron and hole polarons which can be generated optically in $LiNbO_3$. We gained insight to these questions by means of excited-state-absorption (ESA) spectroscopy. Time-resolved measurements of the light-induced absorption in the blue, red, and infrared spectral range upon illumination with intense green laser pulses are shown. The dependencies of α_{li} on the pump beam intensity yield characteristic differences for different degrees of reduction. Based on these findings a self-consistent model is developed taking into account light-induced small electron polarons (Nb_{Nb}^{4+} and Nb_{Li}^{4+}) and hole polarons (O^-), as well as reduction-induced bipolarons ($Nb_{Li}^{4+}:Nb_{Nb}^{4+}$) and residual iron impurities in nominally pure $LiNbO_3$, depending on the degree of reduction. The model considers one-photon dissociation of bipolarons and two-photon generation of hole polarons, both accompanied by the generation of metastable small electron polarons, as well as direct and two-step polaronic recombination processes. We further find evidences for a mutual independence of two-photon hole polaron generation and one-photon dissociation processes of bipolarons, at least for moderate degrees of reduction. These results are of importance for the field of nonlinear optics, since they allow one to adjust the number density of light-induced polarons for two-color holography and for purposes of second-harmonic generation. While the presented model does not directly give quantitative results for the number densities of the involved polarons, these may be calculated from measurements of the light-induced absorption when their respective absorption cross sections are found.

II. EXPERIMENTAL DETAILS

Nominally pure specimens of congruently melting $LiNbO_3$ were purchased from Crystal Technology, Inc. The purity of the samples was controlled by instrumental neutron activation analysis. Besides iron ($c_{Fe}<5$ ppm) no detectable element was found with an impurity level above 1 ppm. The x-cut samples were ground and polished to optical quality. Thermal reduction was performed by vacuum annealing ($p<10^{-4}$ mbar) at different temperatures in the range of 770–1070 K for 6 hours. After this treatment, the crystals had a grayish tint, which is commonly ascribed to the presence of bipolarons (see, e.g., Ref. 22). The corresponding absorption spectra are shown in Fig. 1. As can be seen from the inset, the strength of the bipolaron absorption band depends on the reduction temperature in a strongly nonlinear way. This fact makes it difficult to control the reduction process and may lead to arbitrarily different results for slightly altered experimental conditions. Since the dependence of bipolaron concentration on the reduction conditions in nominally pure $LiNbO_3$ is not known in general, the most convenient characterization is given by the properties of the bipolaron band itself. We will therefore refer to the steady-state absorption at $\lambda=500$ nm, i.e., the maximum of the bipolaron absorption band, as the degree of reduction. A list of the samples used in this work is given in Table I. Measurements of the transient light-induced absorption were performed using a setup for time-resolved ESA spectroscopy. A Q-switched, frequency-doubled Nd:YAG pulse laser ($\lambda=532$ nm, $\tau_{FWHM}=8$ ns, $E_P=300$ mJ) served as the pump light source. The low-intensity probe light of a diode-pumped solid-state laser ($\lambda=488$ nm) and of two semiconductor lasers ($\lambda=785$ nm, 1310 nm), respectively, propagated through the crystal and were simultaneously detected by three PIN diodes. Ordinary light polarization was chosen for pump and probe beams ($\mathbf{e}_p \perp c$ axis). The signals of the diodes were recorded for 20 seconds after the laser pulse with a fast digital storage oscilloscope having a time resolution of 1 ns. After this observation period any light-induced absorption had vanished completely. In order to determine the time-dependent light-induced absorption coefficient $\alpha_{li}(\lambda,t)$ we apply Lambert-Beer's law,

TABLE I. List of the $LiNbO_3$ samples used in this work. The steady-state absorption at $\lambda=500$ nm denotes the degree of reduction.

Sample	T_R (K)	α_{500} (m^{-1})	d (mm)
cln0_2		0	3.19
cln500_1	770	70	1.80
cln550_1	820	100	3.21
cln600_2	870	150	3.20
cln650_1	920	410	3.19
cln700_1	970	760	1.76
cln800_1	1070	1080	1.62

$$I(\lambda,t,d) = I(\lambda,t\leq 0,d=0)\exp[-\alpha(\lambda,t)d]. \quad (1)$$

The absorption coefficient $\alpha(\lambda,t)$ may be written as a sum of the steady-state absorption and the light-induced absorption,

$$\alpha(\lambda,t) = \alpha(\lambda) + \alpha_{li}(\lambda,t). \quad (2)$$

Combining Eqs. (1) and (2) one gets

$$\begin{aligned} I(\lambda,t,d) &= I(\lambda,t\leq 0,d=0)\exp[-\alpha(\lambda)d]\exp[-\alpha_{li}(\lambda,t)d] \\ &= I(\lambda,t\leq 0,d)\exp[-\alpha_{li}(\lambda,t)d], \end{aligned} \quad (3)$$

from which we obtain the formula for the light-induced absorption

$$\alpha_{li}(\lambda,t) = -\frac{1}{d}\ln\left(\frac{I(\lambda,t,d)}{I(\lambda,t\leq 0,d)}\right). \quad (4)$$

The important measures are thus the sample thickness d and the intensities of the transmitted probe light prior to the laser pulse $I(\lambda,t\leq 0,d)$ and after the pulse $I(\lambda,t,d)$.

III. RESULTS

We will first compare the time and intensity dependence of the light-induced absorption for an unreduced (as-grown) sample (cln0_2), a moderately reduced (cln600_2), and a highly reduced sample (cln800_1). Afterwards a comprehen-

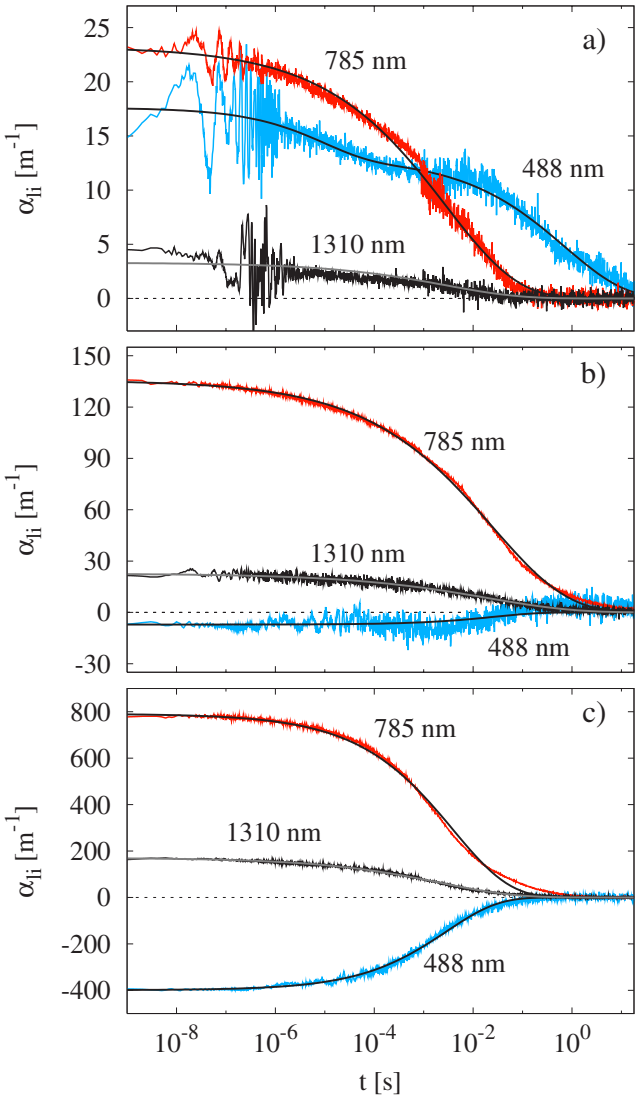

FIG. 2. (Color online) Temporal development of the light-induced absorption for the three probe wavelengths at $T=298$ K: (a) unreduced; (b) reduced at 870 K; (c) reduced at 1070 K. The pump intensity is $I_p=670$ GW/m^2. The solid lines are fits according to Eq. (5).

sive study of the dependence on the degree of reduction is presented. All measurements shown in this work were done at room temperature ($T=298$ K).

A. Time dependence

Figure 2 shows the temporal evolution of the light-induced absorption $\alpha_{li}(t)$ for the three probe wavelengths for an as-grown sample (a), a sample reduced at 870 K (b), and one reduced at 1070 K (c). The pump intensity is $I_p=670$ GW/m^2. In order to visualize the differences between the spectra a logarithmic time scale is used. The signal-to-noise ratio of the data allows a detailed analysis of the decay of $\alpha_{li}(t)$. We find a nonexponential decay behavior, which is best described by stretched exponential functions,[8,20,23–25]

$$\alpha_{li}(t) = \alpha_{li}^{(0)} \exp\left[-\left(\frac{t}{\tau}\right)^{\beta}\right] \tag{5}$$

with the characteristic absorption $\alpha_{li}^{(0)}$, the characteristic lifetime τ, and the stretching factor β. Note that the parameter $\alpha_{li}^{(0)}$ in Eq. (5) must not be mixed up with the amplitude of the light-induced absorption α_{li}^{max}. Although their numerical values may often be very similar, these two quantities are not directly correlated (see also Ref. 24). In all further analyses only the physically meaningful measure α_{li}^{max} is used. The fits according to Eq. (5) are represented by the solid black (gray) lines in Fig. 2. An overview of the fit parameters is given in Table II. In the case of the unreduced sample, one finds a positive light-induced absorption for all three probe wavelengths. The decay of α_{li} exhibits a similar behavior for $\lambda=785$ nm and $\lambda=1310$ nm, yielding a characteristic lifetime of about 3 ms. At $\lambda=488$ nm the decay curve rather yields two components with lifetimes of a few microseconds and close to 1 second, respectively. For reduced $LiNbO_3$ samples we first note remarkably larger values of $\alpha_{li}^{(0)}$. The sign of $\alpha_{li}^{(0)}$ in the blue spectral range becomes negative (b), (c); it is hence denoted as light-induced transparency. Here we find for red, infrared, and blue probe wavelengths similar decay shapes. Their lifetimes are between 2 ms and 30 ms.

B. Intensity dependence

The dependence of the amplitudes of the light-induced absorption α_{li}^{max}, as taken from the time-dependent spectra, on the pump-beam intensity I_p is shown in Fig. 3. For the unreduced sample (a) α_{li}^{max} grows superlinearly with I_p; the fits were obtained assuming the quadratic dependence of Eq. (6). In contrast we find for the highly reduced sample (c) a saturation of the light-induced absorption with increasing pump intensity. This behavior can be satisfactorily described by Eq. (8), yielding the saturation absorption change $\alpha_{li}^{sat}(\lambda)$ and the characteristic intensity $I_S(\lambda)$,

$$\alpha_{li}^{max}(\lambda, I_p) = K(\lambda) I_p^2, \tag{6}$$

$$\alpha_{li}^{max}(\lambda, I_p) = K(\lambda) I_p^2 + \alpha_{li}^{sat}(\lambda)\{1 - \exp[-I_p/I_S(\lambda)]\}, \tag{7}$$

$$\alpha_{li}^{max}(\lambda, I_p) = \alpha_{li}^{sat}(\lambda)\{1 - \exp[-I_p/I_S(\lambda)]\}. \tag{8}$$

The moderately reduced sample (b) shows some peculiarities. First, there is no saturation of α_{li}^{max} for $\lambda=785$ nm. Second, the light-induced transparency in the blue spectral range reaches a maximum at $I_p \approx 200$ GW/m^2, thereafter α_{li}^{max} increases again with I_p. Taken as a whole the behavior of α_{li}^{max} in sample cln600_2 ($T_R=870$ K) resembles that of the highly reduced one for $I_p < 300$ GW/m^2, while for higher intensities a superlinear dependence is observed. The best functional description of the data is therefore achieved by using a sum of a saturation function and a quadratic dependence [Eq. (7)]. A comprehensive summary of the characteristic parameters obtained from Eqs. (6)–(8) is shown in Table III. We note that within the experimental error the quadratic dependence yields the same parameters $K(\lambda)$ for the unreduced and the moderately reduced sample. The characteristic inten-

TABLE II. Parameters obtained from fits of Eq. (5) to the data shown in Fig. 2.

λ (nm)	$\alpha_{\mathrm{li}}^{(0)}$ (m^{-1})	τ (s)	β
cln0_2			
488 fast {slow}	5±2 {13±4}	$(9\pm5)\times10^{-6}$ $\{(7\pm4)\times10^{-1}\}$	0.46±0.05 {0.35±0.05}
785	23±5	$(3\pm1)\times10^{-3}$	0.30±0.05
1310	3±1	$(3\pm1)\times10^{-3}$	0.29±0.05
cln600_2			
488	−7±3	$(3\pm1)\times10^{-2}$	0.48±0.05
785	136±15	$(3\pm1)\times10^{-2}$	0.29±0.05
1310	23±8	$(2\pm1)\times10^{-2}$	0.26±0.05
cln800_1			
488	−400±30	$(3\pm1)\times10^{-3}$	0.42±0.05
785	790±30	$(4\pm2)\times10^{-3}$	0.38±0.05
1310	170±15	$(2\pm1)\times10^{-3}$	0.30±0.05

sities $I_S(\lambda)$ show no wavelength dependence within the experimental error, while their absolute values decrease slightly with the degree of reduction (see also Ref. 26).

C. Reduction dependence

Figure 4 shows the amplitudes of the light-induced absorption versus the degree of reduction for all three probe wavelengths at room temperature and $I_p=670\ \mathrm{GW/m^2}$. The linear dependence is obvious and clarified by fits according to

$$\alpha_{\mathrm{li}}^{\max}(\lambda,\alpha_{500}) = m(\lambda)\alpha_{500} + A(\lambda), \tag{9}$$

with slope $m(\lambda)$, the steady-state absorption α_{500} and the y-axis intercept $A(\lambda)$. The corresponding parameters for all probe wavelengths are listed in Table IV. We find positive slopes for the red and infrared probe wavelengths, while at $\lambda=488$ nm this slope is negative. The zero crossing of the light-induced absorption for $\lambda=488$ nm occurs at $\alpha_{500}\approx130\ \mathrm{m}^{-1}$, which would for the given experimental conditions correspond to a reduction temperature between 820 K (cln550_1) and 870 K (cln600_2).

IV. DISCUSSION

The present work features a systematic study of the light-induced absorption over a wide range of reduction degrees from unreduced (as-grown) to highly reduced samples. Our results support the observations of earlier works,[14,20,23,26] where the existence of light-induced metastable polarons in $LiNbO_3$ has been investigated by means of their related photochromic effects. The pronounced changes in the generation and decay behavior of the light-induced absorption reported in this work, particularly the change of the sign of α_{li}, can be explained straightforwardly by considering the changing interaction of four kinds of light-induced and reduction-induced small polarons.

One may understand the results by separating the temporal and dispersive behavior of the overall absorption $\alpha(\lambda,t)$ into the fundamental absorption $\alpha_0(\lambda)$ and the sum of polaronic absorptions. These can be expressed for each polaronic state i by the sum of a light-independent (steady-state) absorption $\alpha_{0,i}(\lambda)$ and a pump-light-induced absorption change $\alpha_{\mathrm{li},i}(\lambda,t)$. Equation (2) then transforms to

$$\alpha(\lambda,t) = \alpha_0(\lambda) + \sum_i [\alpha_{0,i}(\lambda) + \alpha_{\mathrm{li},i}(\lambda,t)], \tag{10}$$

where the light-independent summands correspond to $\alpha(\lambda)$ and the light-induced summands to $\alpha_{\mathrm{li}}(\lambda,t)$ in Eq. (2), respectively. The absorption spectra in Fig. 1 reflect the case where $\alpha_{\mathrm{li},i}(\lambda,t)=0$. An influence of the pump pulse on the fundamental absorption is neglected, i.e., we assume that optically induced damages of the crystal lattice or of the optical properties of bulk and surface do not occur. This assumption is fairly well justified since the light-induced absorption completely vanished in all of our experiments after a few seconds (cf. Fig. 2). Furthermore, microscopic inspections of the sample surfaces did not reveal any changes. A second assumption is that we take into account the presence of four polaronic states i contributing to our signals. The respective steady-state number densities are denoted by $N_{0,i}$ and the light-induced density changes by $N_{\mathrm{li},i}(t)$. Together with the absorption cross sections $\sigma_i(\lambda)$ the polaronic absorption is written as

$$\sum_i [\alpha_{0,i}(\lambda) + \alpha_{\mathrm{li},i}(\lambda,t)] = \sum_i [N_{0,i}\sigma_i(\lambda) + N_{\mathrm{li},i}(t)\sigma_i(\lambda)]. \tag{11}$$

Changes in $\alpha(\lambda,t)$ are therefore unambiguously attributed to changes of the particular number densities of polaronic states $N_{\mathrm{li},i}(t)$. It is thus clear that an increase of one center's number density $[N_{\mathrm{li},i}(t)>0]$ with simultaneous decrease of the number density of another center $[N_{\mathrm{li},j}(t)<0]$ can result in a competing photochromic effect, given that both centers have similar absorption cross sections in a certain wavelength range. In the following we will refer to this increase and decrease as *generation* and *depopulation*, respectively.

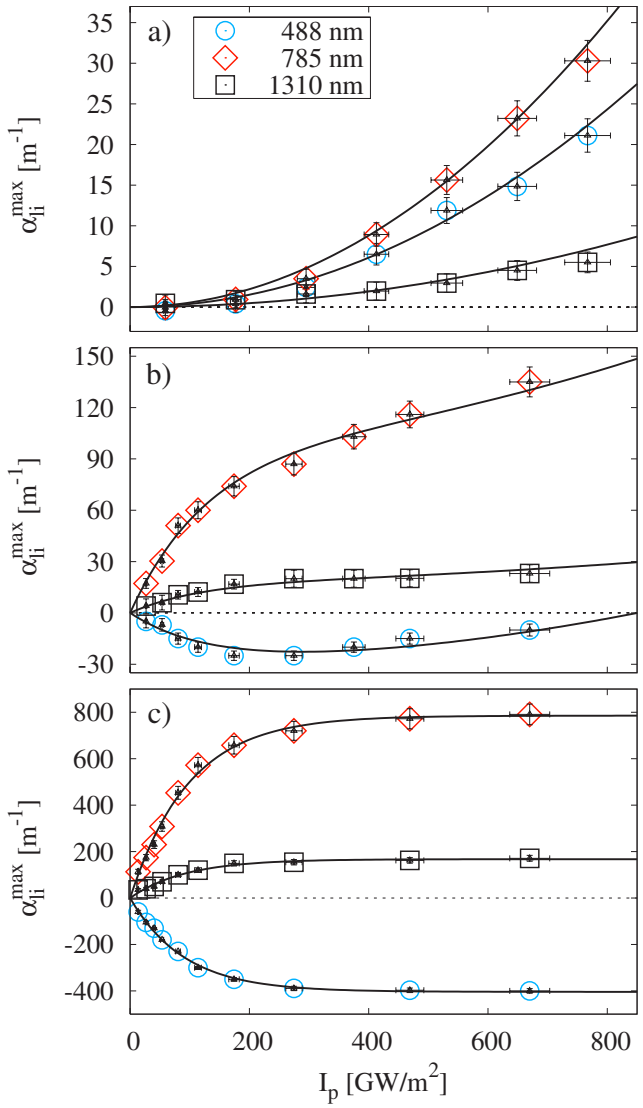

FIG. 3. (Color online) Amplitudes of the light-induced absorption versus pump intensity for the three probe wavelengths at T =298 K: (a) unreduced; (b) reduced at 870 K; (c) reduced at 1070 K. The lines are fits of (a) Eq. (6), (b) Eq. (7), and (c) Eq. (8), respectively.

A. Build-up and decay kinetics of $\alpha_{li}(t)$

All light-induced absorption changes reach their maximum values α_{li}^{max} within the duration of the pump pulse in any sample and under any pump-probe condition. That means that the processes of dissociation and generation of small polarons—resulting in the respective number densities $N_{li,i}(t)$—are faster than nanoseconds; they can therefore not be resolved temporally with our experimental setup. In fact, the time constants for optical generation of small polarons in $LiNbO_3$ were reported to be less than 10^{-12} s.[27,28] However, an indirect insight to the excitation processes can be revealed from the obtained values of the light-induced absorption immediately after exposure, $\alpha_{li,i}(\lambda, t=0)$, from its sign, its dispersive behavior and its intensity dependence, respectively (see Figs. 2 and 3).

TABLE III. Parameters obtained from fits of Eqs. (6)–(8) to the data shown in Fig. 3.

λ (nm)	K (10^{-6} m^3/GW^2)	α_{li}^{sat} (m^{-1})	I_S (GW/m^2)
cln0_2			
488	38±10		
785	55±15		
1310	12±5		
cln600_2			
488	40±10	−28±5	126±15
785	65±15	103±15	134±15
1310	15±5	19±4	121±15
cln800_1			
488		−405±25	91±8
785		790±40	99±9
1310		167±12	92±8

After excitation, the carriers' recombination, i.e., the decrease of $N_{li,i}(t)$, happens with time constants from microseconds to seconds (cf., for instance, Ref. 24). This recombination is accompanied by a decay of the light-induced absorption which is reflected by the characteristic transient spectra shown in Fig. 2. The apparently nonexponential decay behavior of $\alpha_{li}(t)$ in $LiNbO_3$ has been mentioned before[8,20,23–25] and stretched exponential functions have been applied instead [cf. Eq. (5)]. Possible explanations for this effect include thermal disorder of the material,[24] direct long-range transitions between centers,[8,23] and hopping charge transport.[25,29] Small polaron theory on its part implies hopping transitions between nearest-neighbor sites as the main charge transport mechanism at room temperature and above.[11–13] Despite the fact that none of the above-mentioned

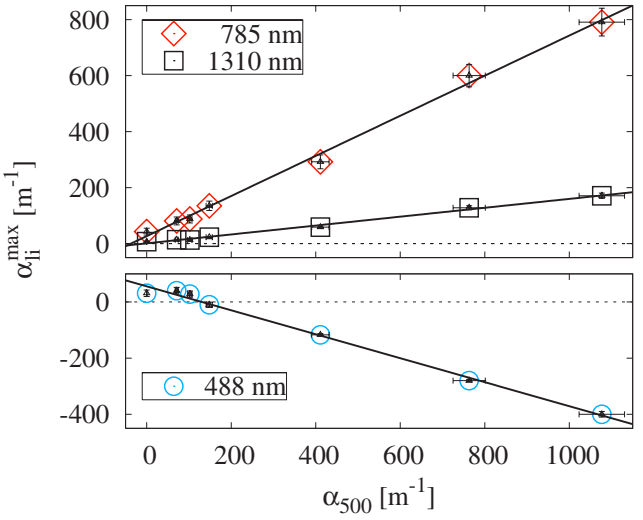

FIG. 4. (Color online) Amplitudes of the light-induced absorption versus degree of reduction for the three probe wavelengths at T=298 K and a pump intensity of I_p=670 GW/m^2. The solid lines are linear fits according to Eq. (9).

TABLE IV. Parameters obtained from fits of Eq. (9) to the data shown in Fig. 4.

λ (nm)	m	A (m^{-1})
488	−0.42±0.05	55±25
785	0.72±0.08	27±15
1310	0.16±0.05	1±5

theories directly yields a stretched exponential decay, recent numerical simulations have shown that for the time being nearest-neighbor hopping of free small Nb_{Nb}^{4+} polarons seems to be the most convenient explanation for the nonexponential decay behavior of $\alpha_{li}(t)$ in $LiNbO_3$.[30]

The experimental data are further analyzed with respect to the optical excitation and thermal recombination processes, and the model depicted in Fig. 5 is deduced. We particularly distinguish between unreduced (as-grown) and reduced samples which are individually discussed in detail in the following.

B. Unreduced $LiNbO_3$

Positive light-induced absorption changes in nominally pure, unreduced $LiNbO_3$ were previously assigned to the generation of bound O^- hole polarons and bound Nb_{Li}^{4+} electron polarons.[14,20] A quadratic dependence of α_{li} on the pump intensity was found at λ=488 nm,[20] which affirmed the previously assumed two-photon process.[14] We also clearly observe a quadratic dependence, not only at λ=488 nm, but at all probe wavelengths used in our investigation. Furthermore, we find a longer lifetime of α_{li} at λ=488 nm, compared to that in the red and infrared spectral range. The complete process of excitation and relaxation of the light-induced absorption in as-grown $LiNbO_3$ can be explained using the model of Herth *et al.*,[20] which is shown in the left half of Fig. 5. Electrons are excited from the valence band to the conduction band via a two-photon process, leaving a hole in the valence band. The carriers form small electron polarons at Nb_{Nb} and Nb_{Li} sites $[N_{li,Nb_{Nb}^{4+}}(t), N_{li,Nb_{Li}^{4+}}(t) > 0]$ (Ref. 22) as well as bound small hole polarons at oxygen ions adjacent to a lithium vacancy $[N_{li,O^-}(t) > 0]$.[14,21] The characteristic lifetimes of the decay $\alpha_{li}(t)$ suggest that one single relaxation process is observed in the red and infrared spectral range, most likely the recombination of Nb_{Li}^{4+} and O^- polarons. In this case the light-induced absorption at λ=1310 nm is due to the infrared tail of the bound-polaron absorption.[24] The different shape and remarkably longer lifetime of α_{li} at λ=488 nm can, however, not be explained in this simple manner. A sole interaction of Nb_{Li}^{4+} and O^- would essentially result in identical decay shapes for all probe wavelengths, so an additional center must be postulated, which need not necessarily be photochromic in itself. It only must be a sufficiently deep electron trap. Therefore, the most reasonable responsible center is the residual extrinsic $Fe^{2+/3+}$ impurity. During the relaxation process a certain amount of electrons can be trapped as Fe^{2+}, enhancing the absorption at λ=488 nm.[20] The characteristic time for this process is reported to be a few microseconds,[20] a value that coincides with the lifetime of the first decay component in our investigations (cf. Table II). After all electron polarons have recombined a good part of the hole polaron population remains. The recombination of electrons from Fe^{2+} with the O^- hole polarons proceeds much slower due to larger binding energies.[31] Herth *et al.* found lifetimes around 1 s for the second decay component in $LiNbO_3$:Fe at λ=488 nm.[20] If iron impurities are responsible for this effect, they should also affect the excitation process. We consider a possible excitation of electrons from Fe^{2+} to the conduction band (see Fig. 5).[20] However, since in unreduced $LiNbO_3$ samples the ratio $N_{Fe^{2+}}/N_{Fe^{3+}}$ is generally much smaller than unity, while the total Fe concentration is extremely low, this one-photon process may not be visible in our case. The fact that we do not observe an additional increase of α_{li} at λ=488 nm—as Herth *et al.* did in Fe-doped samples[20]—supports this interpretation. From the data shown in Fig. 2(a) one may roughly

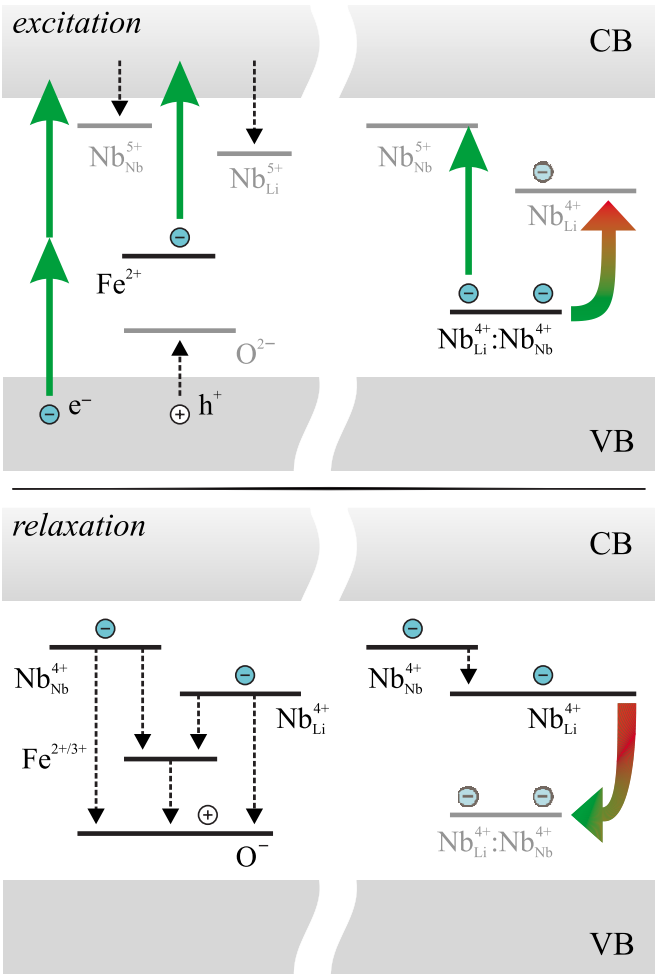

FIG. 5. (Color online) Schematic description for the different mechanisms of excitation and generation (upper graphic) and recombination and depopulation (lower graphic) of small polarons in unreduced (left half) and reduced $LiNbO_3$ (right half). Thick arrows denote excitations by pump light, dashed arrows denote thermal relaxations. Bent thick arrows stand for the transformation of states without electronic transitions. Note that the energy levels are shown only schematically; they do not represent absolute defect energies.

estimate the upper limit of the Fe^{2+}-related light-induced absorption as α_{li} (488 nm, Fe^{2+}) $< 10\ m^{-1}$. Using the relations given in Ref. 32 we obtain the number density of metastable Fe^{2+} ions as $N_{li,Fe^{2+}} < 2 \times 10^{22}\ m^{-3} \hat{=} 1$ ppm. This upper bound is in good agreement with the reported total iron concentration ($c_{Fe} < 5$ ppm). The role of free small Nb_{Nb}^{4+} polarons in unreduced material on the other hand is not clear. Recent measurements indicate their influence at least in reduced samples, especially for lower pump intensities.[25] We have therefore included the Nb_{Nb}^{4+} state in our model, also because it is the main electron transport state in $LiNbO_3$.

C. Reduced $LiNbO_3$

The broad absorption band centered at $\lambda = 500$ nm and appearing upon thermal reduction in nominally pure $LiNbO_3$ shown in Fig. 1 was assigned to the presence of Nb_{Li}^{4+}:Nb_{Nb}^{4+} bipolarons by optical and ESR spectroscopy.[15,16,33] Since in undoped material these states represent the energetically lowest level, they are stable at room temperature. For the case of nominally pure, reduced samples, we therefore must take into account the polaronic steady-state absorption $\alpha_{0,i}(\lambda) > 0$. Illumination with light in the blue-green spectral range leads to a dissociation of the bipolarons $[N_{li,Nb_{Li}^{4+}:Nb_{Nb}^{4+}}(t) < 0]$ in favor of metastable small Nb_{Li}^{4+} bound polarons.[16,22,26] The corresponding model is depicted in the right half of Fig. 5. According to the theory for small polarons as given by Emin,[19] this kind of dissociation should excite one of the electrons to an adjacent Nb site, resulting in the formation of a free small Nb_{Nb}^{4+} polaron $[N_{li,Nb_{Nb}^{4+}}(t) > 0]$. The second electron ($Nb_{Li}^{4+}$:$Nb_{Nb}^{5+}$) remains as a bound small Nb_{Li}^{4+} polaron $[N_{li,Nb_{Li}^{4+}}(t) > 0]$. This transformation of the state is not accompanied by an electronic transition, and is denoted by the bent arrow in Fig. 5. Although there is to date no definite experimental proof for light-induced free polarons in reduced $LiNbO_3$, an evidence that it is correct to apply Emin's theory[19] in this context has been shown only recently.[25] The optical dissociation of bipolarons is a one-photon process, resulting in a linear growth of the absolute amplitudes of α_{li} for small pump intensities.[26] In accordance with Jermann *et al.* we find a saturation of the light-induced absorption for high values of I_p.[26] The saturation of α_{li}^{max} indicates that the generation of small polarons is limited by the number density of bipolarons $N_{0,BP}$. This interpretation is further supported by the linear dependence of the amplitudes α_{li}^{max} on the equilibrium absorption at $\lambda = 500$ nm, which is directly related to $N_{0,BP}$ (see Fig. 4). Like in the as-grown sample, we find a consistence of the fit parameters $K(\lambda)$ and $\alpha_{li}^{sat}(\lambda)$ in the red and infrared spectral range,

$$\frac{K(785\ \text{nm})}{K(1310\ \text{nm})}(\text{cln0\_2}, \text{cln600\_2}) \approx \frac{\alpha_{li}^{sat}(785\ \text{nm})}{\alpha_{li}^{sat}(1310\ \text{nm})}(\text{cln600\_2}, \text{cln800\_1}) \approx 4.5 - 5.5.$$

From this observation we might conclude that one single process is observed for both probe wavelengths: generation and depopulation of bound small Nb_{Li}^{4+} polarons.[26] It has, however, been shown that the polaronic recombination process in reduced $LiNbO_3$ is not governed by Nb_{Li}^{4+} polarons alone. One rather finds that in the low-intensity regime (linear $\alpha_{li}^{max} - I_p$ dependence, cf. Fig. 3) two recombination paths are taken.[25] The first of these was identified as a direct recombination of Nb_{Nb}^{4+} and Nb_{Li}^{4+} polarons, yielding lifetimes in the microsecond range. In the second case the electrons are intermediately trapped at Nb_{Li}^{5+} centers, which leads to longer lifetimes of several milliseconds. We believe that this second path is mainly taken in the saturation regime shown in the present work. The reasons for this behavior are to date still unclear. One possible explanation may be a pronounced generation of bound polarons at higher pump intensities, caused by multiple excitations within the pulse duration.[30] Eventually, an involvement of $Fe^{2+/3+}$ in the recombination (and excitation) process in reduced $LiNbO_3$ would yield much weaker effects than the polaronic one (see Fig. 3); it can thus be safely neglected for highly reduced samples.

D. Moderately reduced $LiNbO_3$

In the case of moderately reduced samples we must consider all of the effects and mechanisms described above. For certain experimental conditions (degree of reduction, pump intensity, sample temperature) one can even find a vanishing photochromic effect in the blue wavelength range. At the same time the amplitudes of α_{li} in the red and infrared grow steadily with increasing intensity and degree of reduction, indicating that the generation of small electron polarons still takes place (cf. Fig. 4). Moreover, for moderate pump intensities the light-induced absorption resembles that of reduced samples, while for higher intensities the characteristics rather correspond with unreduced $LiNbO_3$ (see Fig. 3). The explanation that no effects occur in moderately reduced samples is therefore not tenable. It is known that bipolarons and hole polarons are accompanied by very similar absorption bands in $LiNbO_3$.[14,21] Therefore, considering the remarks given above, we must assume that the two processes of bipolaron dissociation and hole-polaron generation—as depicted in Fig. 5—take place simultaneously. As can be seen from Eqs. (10) and (11) a competing photochromic effect in the blue spectral range obviously results in this case, leaving the light-induced absorption in the red and infrared widely unaffected. The fact that the quadratic parameters $K(\lambda)$ for the unreduced and moderately reduced sample are almost identical further supports this conclusion. However, the mutual independence of the processes described here holds only as a first approximation. For example, the one-photon dissociation of bipolarons is by far the most probable process and results in a reduced photon flux inside the sample. As a consequence the generation of hole polarons, which depends on a two-photon process, is heavily restrained. More complex effects, like multiple steps of generation and depopulation of the different polaronic states, might occur during the excitation process (see Ref. 30). A decisive answer to this question cannot be given by the presented results.

V. SUMMARY AND CONCLUSIONS

We have shown time-resolved measurements of the light-induced absorption upon illumination with intense green la-

ser pulses in nominally pure, as-grown and reduced congruently melting lithium niobate. Our observations for unreduced and highly reduced material are in full accordance with previous reports.[14,20,26] From the positive transient light-induced absorption $\alpha_{li}(t)$ in the blue, red, and infrared spectral range we can conclude that the two-photon-induced generation of free and bound small Nb_{Nb}^{4+} and Nb_{Li}^{4+} electron polarons and bound small O^- hole polarons is observed in unreduced $LiNbO_3$. The recombination of electron and hole polarons in the dark is partly affected by $Fe^{2+/3+}$ centers which act as intermediate electron traps and lead to a longer lifetime of $\alpha_{li}(t)$ in the blue spectral range. One may take an upper-bound value of less than 1 ppm as a rough estimate of metastable Fe^{2+} ions involved in the process. In reduced material we observe the one-photon-induced dissociation of small $Nb_{Li}^{4+}:Nb_{Nb}^{4+}$ electron bipolarons, resulting in a light-induced transparency in the blue spectral range. The simultaneous generation of small electron polarons yields a positive light-induced absorption in the red and infrared. A possible influence of residual Fe impurities on the excitation and recombination behavior of Nb_{Nb}^{4+} and Nb_{Li}^{4+} is a minor effect and may in this case be neglected. In the intermediate reduction regime both dissociation of bipolarons and generation of hole polarons take place, leaving the generation of small electron polarons virtually unaffected. While therefore the photochromic effects in the red and infrared spectral range grow linearly with the degree of reduction of the samples, they pass a zero crossing in the blue spectral range. Recent investigations further indicate a crucial influence of free small Nb_{Nb}^{4+} polarons on the above-mentioned processes in $LiNbO_3$. The nonexponential decay of the light-induced absorption changes implies a spatial charge transport whose nature is not completely understood; the most reasonable explanation to date is nearest-neighbor hopping of free small Nb_{Nb}^{4+} polarons.

A self-consistent model for the light-induced dissociation, generation, and recombination processes of small polarons in nominally pure lithium niobate has been presented in this work. From these comprehensive findings follows a controllability of the particular number densities of small polarons in $LiNbO_3$. This feature is interesting for photosensitive applications, including the reduction of thermo-optical damage during frequency conversion and tailoring of the material for two-color holography. Once the absorption cross sections of the involved polarons are found, one may even directly calculate their number densities from measurements of the light-induced absorption.

ACKNOWLEDGMENTS

The authors would like to thank W. Geisler for preparation of the $LiNbO_3$ samples and G. Cornelsen for the reduction treatment and measurements of the steady-state absorption. The authors also thank Th. Woike for performing the INA analysis and M. Wöhlecke and O. F. Schirmer for fruitful discussions. Financial support by the Deutsche Forschungsgemeinschaft (Contracts Nos. IM 37/2-1 and TFB 13-04) is gratefully acknowledged.

*cmerschj@uos.de

[1] K. Buse, F. Jermann, and E. Krätzig, Opt. Mater. (Amsterdam, Neth.) **4**, 237 (1995).
[2] Y. S. Bai and R. Kachru, Phys. Rev. Lett. **78**, 2944 (1997).
[3] L. Hesselink, S. Orlov, A. Liu, A. Akella, D. Lande, and R. Neurgaonkar, Science **282**, 1089 (1998).
[4] H. Günther, R. Macfarlane, Y. Furukawa, K. Kitamura, and R. Neurgaonkar, Appl. Opt. **37**, 7611 (1998).
[5] Y. Furukawa, S. A. Markgraf, M. Sato, H. Yoshida, T. Sasaki, H. Fujita, and T. Yamanaka, Appl. Phys. Lett. **65**, 1480 (1994).
[6] M. P. Scripsick, X. H. Fang, G. H. Edwards, L. E. Halliburton, and J. K. Tyminski, J. Appl. Phys. **73**, 1114 (1993).
[7] S. D. Setzler, K. T. Stevens, N. C. Fernelius, M. P. Scripsick, G. J. Edwards, and L. E. Halliburton, J. Phys.: Condens. Matter **15**, 3969 (2003).
[8] S. Wevering, J. Imbrock, and E. Krätzig, J. Opt. Soc. Am. B **18**, 472 (2001).
[9] H. Mabuchi, E. S. Polzik, and H. J. Kimble, J. Opt. Soc. Am. B **11**, 2023 (1994).
[10] Y. Furukawa, K. Kitamura, A. Alexandrowski, R. K. Route, M. M. Fejer, and G. Foulon, Appl. Phys. Lett. **78**, 1970 (2001).
[11] T. Holstein, Ann. Phys. **8**, 325 (1959).
[12] T. Holstein, Ann. Phys. **8**, 343 (1959).
[13] I. G. Austin and N. F. Mott, Adv. Phys. **18**, 41 (1969).
[14] O. F. Schirmer and D. von der Linde, Appl. Phys. Lett. **33**, 35 (1978).
[15] J. Koppitz, O. F. Schirmer, and A. I. Kuznetsov, Europhys. Lett. **4**, 1055 (1987).
[16] O. F. Schirmer, S. Juppe, and J. Koppitz, Cryst. Lattice Defects Amorphous Mater. **16**, 353 (1987).
[17] B. Faust, H. Müller, and O. F. Schirmer, Ferroelectrics **153**, 297 (1994).
[18] D. M. Smyth, Ferroelectrics **50**, 419 (1983).
[19] D. Emin, Phys. Rev. B **48**, 13691 (1993).
[20] P. Herth, T. Granzow, D. Schaniel, T. Woike, M. Imlau, and E. Krätzig, Phys. Rev. Lett. **95**, 067404 (2005).
[21] O. F. Schirmer, J. Phys.: Condens. Matter **18**, R667 (2006).
[22] O. F. Schirmer, O. Thiemann, and M. Wöhlecke, J. Phys. Chem. Solids **52**, 185 (1991).
[23] D. Berben, K. Buse, S. Wevering, P. Herth, M. Imlau, and T. Woike, J. Appl. Phys. **87**, 1034 (2000).
[24] P. Herth, D. Schaniel, T. Woike, T. Granzow, M. Imlau, and E. Krätzig, Phys. Rev. B **71**, 125128 (2005).
[25] C. Merschjann, D. Berben, M. Imlau, and M. Wöhlecke, Phys. Rev. Lett. **96**, 186404 (2006).
[26] F. Jermann, M. Simon, R. Böwer, E. Krätzig, and O. F. Schirmer, Ferroelectrics **165**, 319 (1995).
[27] O. Beyer, D. Maxein, K. Buse, B. Sturman, H. T. Hsieh, and D. Psaltis, Opt. Lett. **30**, 1366 (2005).
[28] Y. Qiu, K. B. Ucer, and R. T. Williams, Phys. Status Solidi C **2**, 232 (2005).
[29] B. Sturman, E. Podivilov, and M. Gorkunov, Phys. Rev. Lett. **91**,

176602 (2003).
[30] J. Carnicero, M. Carrascosa, G. García, and F. Agulló-López, Phys. Rev. B **72**, 245108 (2005).
[31] A. Zylbersztejn, Appl. Phys. Lett. **29**, 778 (1976).
[32] H. Kurz, E. Krätzig, W. Keune, H. Engelmann, U. Gonser, B. Dischler, and A. Räuber, Appl. Phys. **12**, 355 (1977).
[33] D. A. Dutt, F. J. Feigl, and G. G. DeLeo, J. Phys. Chem. Solids **51**, 407 (1990).